Investigating Cytochrome P450 specificity during Glycopeptide Antibiotic biosynthesis through a homologue hybridization approach

Clara Brieke [a#], Miroslaw Tarnawski [a#], Anja Greule [b, c] and Max J. Cryle [a, b, c*]

[a] Department of Biomolecular Mechanisms, Max Planck Institute for Medical Research, Jahnstrasse 29, 69120 Heidelberg, Germany.

[b] The Monash Biomedicine Discovery Institute, Department of Biochemistry and Molecular Biology, Monash University, Clayton, Victoria 3800, Australia. EMBL Australia, Monash University, Clayton, Victoria 3800, Australia.

[c] ARC Centre of Excellence in Advanced Molecular Imaging, Monash University, Clayton, Victoria 3800, Australia.

[#] Authors contributed equally to this work.

* Address correspondence to Max.Cryle@monash.edu; Tel. +61 3 9905 0771.

Abstract

Cytochrome P450 enzymes perform an impressive range of oxidation reactions against diverse substrate scaffolds whilst generally maintaining a conserved tertiary structure and active site chemistry. Within secondary metabolism, P450 enzymes play widespread and important roles in performing crucial modifications of precursor molecules, with one example of the importance of such reactions being found in the biosynthesis of the glycopeptide antibiotics (GPAs). In GPA biosynthesis P450s, known as Oxy enzymes, are key players in the cyclization of the linear GPA peptide precursor, which is a process that is both essential for their antibiotic activity and is the source of the synthetic challenge of these important antibiotics. In this work, we developed chimeric P450 enzymes from GPA biosynthesis based on two homologues from different GPA biosynthesis pathways – vancomycin and teicoplanin – as an approach to explore the divergent catalytic behavior of the two parental homologues. We could generate, crystalize and explore the activity of new hybrid P450 enzymes from GPA biosynthesis and show that the unusual *in vitro* behavior of the vancomycin OxyB homologue does not stem from the major regions of the P450 active site, and that additional regions in and around the P450 active site must contribute to the unusual properties of this P450 enzyme. Our results further show that it is possible to successfully transplant entire regions of secondary structure between such P450s and retain P450 expression and activity, which opens the door to use such targeted approaches to generate and explore novel biosynthetic P450 enzymes.

Introduction

Natural product biosynthesis is of great importance for society, where it provides a significant source of bioactive compounds.[1] Within natural product biosynthesis pathways, it is common to find members of the Cytochrome P450 monooxygenase superfamily: these enzymes display a truly staggering capacity to perform varied oxidative chemistry against widely differing substrate structures.[2] Perhaps even more impressively, this diversity of reactivity and substrate scope is maintained within a highly conserved three-dimensional fold and reaction cycle.[2] Given the utility of P450s in complex biosynthesis pathways, the possibility to use P450s as biocatalysts has received significant attention in the field.[3] Furthermore, the ability to alter the substrate specificity or reaction region/stereoselectivity via targeted mutagenesis or enzyme evolution approaches has made P450s attractive targets for enzyme engineering and synthetic biology. Approaches that have been used to "hybridize" P450 enzymes includes the highly successful use of restriction-digest based methods followed by screening of the resultant P450 libraries for mammalian P450s: such approaches have identified hybrid P450s displaying specificity for substrates that is not found in either parental template, indicating the potential for uncovering novel P450s through hybridization.[4-8]

Whilst approaches used in P450 reengineering have generated important examples of diversified biocatalysts, less attention has been paid to the ability to affect large changes in P450 structure – and possibly activity – through the exchange of complete secondary structure elements within the P450 fold. To explore whether such an approach is viable for P450 redesign, we set out to test the ability to exchange active site elements from P450 enzymes from bacterial glycopeptide antibiotic biosynthesis.[9-11] We chose this system due to the importance of the P450-mediated transformations performed during glycopeptide antibiotic (GPA) biosynthesis, where a cascade of three to four P450s act sequentially to cyclize linear GPA precursor peptides via the oxidative coupling of aromatic side chains to afford GPA peptides in their fully crosslinked, active form (Figure 1).[10, 12-15] *In vitro* studies to date have indicated that the first P450 enzyme in the oxidative cascade, OxyB, can display a wide range of activities that differ in both the substrate peptide structure and also in the acceptance of alternate constructs from the peptide-producing non-ribosomal peptide synthetase (NRPS) machinery.[16-27]

One of the most widely studied examples of an OxyB homologue is $OxyB_{van}$ from the vancomycin biosynthetic gene cluster.[24-26] This P450 has been demonstrated to possess a high tolerance for altered peptide substrates, includes the acceptance of peptides ranging in length from three to seven amino acids and also a range of hexapeptides and heptapeptides displaying modified N-terminal peptide sequences that match to all other classes of glycopeptide antibiotics reported to date.[19-22, 24-27] $OxyB_{van}$ is able to catalyze side chain crosslinking

to a high level of peptides presented by the carrier protein domain from module seven of the vancomycin NRPS and has also demonstrated activity against peptides bound to peptidyl carrier protein (PCP)-domains from other glycopeptide antibiotic NRPS machineries.[16-27] Recently, we have shown that the previously enigmatic X-domain found in the terminal module of all GPA peptide producing NRPS machineries is a general recruitment and interaction platform for Oxy enzymes to interact with the peptide bound PCP-domain.[19] The X-domain maintains the fold of a peptide-bond forming condensation domain, but bears mutations that render this domain catalytically silent in terms of peptide synthesis.[19] Rather, the X-domain serves to recruit all P450 enzymes responsible for peptide cyclization during GPA biosynthesis, which functions via the constant cycling of the P450s bound to the X-domain in order to scan the crosslinking state of the neighboring PCP-domain and maintain an effective peptide crosslinking process.[18] The X-domain binds to the Oxy enzymes via electrostatic and hydrogen bond-mediated interactions focused on the F- and G-helices of these P450s – particularly crucial to the P450/X-domain interaction is the conserved PRDD motif found at the start of the F-helix, with mutation of the residues in the X-domain that contact this motif leading to a loss of interaction as well as resultant peptide cyclization activity by the P450s.[19] The X-domain has also been demonstrated *in vitro* to be essential for the reconstitution of the Oxy enzymes responsible for insertion of the D-*O*-E and F-*O*-G rings into GPA peptides (performed by OxyA and OxyE, see Figure 1),[18-20, 28] although the importance of the X-domain with regards the initial insertion of the C-*O*-D ring by the P450 OxyB is less clear. In the case of $OxyB_{van}$ the presence of the X-domain was also shown to improve *in vitro* peptide crosslinking albeit at significantly reduced levels when compared to other systems, although these differences become more significant with alterations to the peptide (such as chlorination).[16, 19, 23]

In contrast to the broad substrate specificity displayed by $OxyB_{van}$, OxyB from teicoplanin biosynthesis ($OxyB_{tei}$) displays a much narrower range of activity concerning the substrate peptide and mode of presentation: this results in a reduction in activity when the peptide structure is altered from that of teicoplanin, with the reduction in activity correlating with the divergence of the peptide structure from that of teicoplanin.[19, 20, 22] $OxyB_{tei}$ activity is highly dependent upon the presence of the X-domain, with peptides presented on isolated PCP-domains shown to be poor substrates in peptide cyclization experiments *in vitro*.[19, 22] What makes the significant differences in activity between $OxyB_{tei}$ and $OxyB_{van}$ all the more intriguing is that these enzymes share a very high sequence identity (74% sequence identity) as well as structural similarity (RMSD 1.3 Å).[22, 29] In an attempt to understand the reasons for these differences, we decided to construct a series of modified $OxyB_{tei}$ enzymes in which large structural elements of the P450 active sites were transplanted from $OxyB_{van}$ to create chimeric Oxy proteins, whose properties could then be

analyzed and compared to the two parental OxyB homologues. Furthermore, this study would shed light on the extent to which chimeric P450 enzymes could be constructed using a rational approach based on the exchange of large structural elements within these P450s, which is potential approach to explore P450 activity, selectivity and generate P450 chimeras displaying potentially novel properties.

Experimental

Construct design and cloning. Three genes encoding the OxyB hybrid proteins $OxyB_{tei\_BCv}$, $OxyB_{tei\_FGv}$ and $OxyB_{tei\_BC/FGv}$ were obtained as synthetic genes that had been codon optimized for *E. coli* expression (Eurofins Genomics). Protein sequences were taken from that of $OxyB_{tei}$, with the following residue ranges switched for the corresponding sequence of the vancomycin homologue: $OxyB_{tei\_BCv}$ (residues 56-94 from $OxyB_{van}$), $OxyB_{tei\_FGv}$ (residues 158-203 from $OxyB_{van}$) and $OxyB_{tei\_BC/FGv}$ (residues 56-94 and 158-203 from $OxyB_{van}$). The genes were designed containing 5'-NdeI (in frame with start-Met) and 3'-HindIII restriction sites (following two stop codons) for a standard restriction enzyme/ ligation cloning strategy into the pET28a expression vector (Novagen). Following cloning, constructs were then verified by sequencing using standard primers; the resultant constructs contain an N-terminal 6xHis tag and thrombin protease cleavage site prior to the start methionine of the Cytochrome P450.

Protein Expression, Purification and Characterization. Expression and purification of the OxyB hybrid enzymes generally followed the established protocol for the parental enzyme $OxyB_{tei}$.[19, 20, 22] Briefly, 1% (v/v) of an overnight culture of BL21(DE3) cells containing the relevant P450 expression plasmid was used to inoculate LB- or TB-media supplemented with kanamycin (50 mg/L). The cultures were then incubated with gentle shaking at 37°C until an OD_{600} of ~0.5 was reached. The temperature was then reduced to 18°C and the media supplemented with the heme-precursor δ-aminolevulinic acid. Protein expression was then induced at an OD_{600} of ~1.0 through the addition of IPTG (0.1 mM) and incubation continued at 18°C for 16 h. Purification of the hybrid enzymes was performed through initial Ni^{2+}-NTA (nitrilotriacetic acid agarose resin) affinity chromatography to isolate the crude protein, followed by overnight buffer exchange prior to anion exchange chromatography. A final polishing step was performed using gel filtration, which afforded hybrid OxyB enzymes in a purity of >95% as assessed by SDS-PAGE, whilst the identity of the proteins was confirmed through the use of peptide mass fingerprinting. Yields of the two hybrid enzymes that were purified to completion were 160 nmol/L for the $OxyB_{tei\_FGv}$ hybrid (optimal expression in LB media) and 110 nmol/L for the $OxyB_{tei\_BC/FGv}$ hybrid (optimal expression in TB media). NRPS-derived carrier protein constructs (PCP_7-X_{tei} (teicoplanin biosynthesis), PCP_{7_com} (complestatin biosynthesis), PCP_{7_tei} (teicoplanin biosynthesis), PCP_{7_cep} (chloroeremomycin

biosynthesis)) were expressed and purified as has been previously reported.[19-22] Spectra were obtained using a Jasco V-750 spectrophotometer. The OxyB enzymes were diluted to 2.5 μM in Tris-HCl (50 mM, pH 7.4) and the UV/Vis spectra was measured at 30°C between 390-600 nm. The enzymes were reduced using 10 μL of a saturated sodium hydrosulfite (Sigma) solution and CO was generated by adding a small amount of disodium boranocarbonate (Dalton Pharma Service) to the enzyme solution

Crystallization, Structural Characterization and Alignment. The $OxyB_{tei\_BC/FGv}$ hybrid was crystallized using the hanging-drop vapor diffusion method by mixing 1 μL of protein (7 mg/mL protein in buffer (0.1 M Tris-HCl (pH 7.4) and 0.15 M NaCl)) with 1 μL of reservoir solution containing 0.1 M Na Hepes (pH 7.5), 0.2 M KAc and 20% PEG 3350. Crystals (plates ~ 100 μM in length) formed over a period of a week at 20°C. Crystals were passed through the reservoir solution supplemented with 20% glycerol and flash-cooled in liquid nitrogen. Diffraction data were collected at the SLS (beamline X10SA) with the crystal kept at 100 K and were processed using the XDS program suite.[30] The crystal is in space group P1 with four P450 molecules per asymmetric unit, with phasing accomplished using Phaser[31] and a search model based on $OxyB_{tei}$ (PDB Code 4TVF) with the altered regions of the structure trimmed. During rounds of manual rebuilding in Coot[32, 33] and refinement with Phenix (non-crystallographic symmetry (NCS) restraints were included during refinement and the following TLS groups were used for chain A: 7-157, 158-221, 222-398 and chains B, C, D: 7-159, 160-221, 222-398.),[34] the majority of amino acid residues as well as heme and solvent molecules were included in the model. Model quality was assessed using Molprobity.[35] Structure-based sequence alignments were carried out with SSM[36] as implemented in Coot,[32, 33] with comparisons to known structures performed using the Dali server.[37] Sequence alignment were performed using Clustal Omega,[38] and assessment of peptide aliphatic indices were made using ProtParam.[39] All structural figures were prepared using PyMol.[40]

Synthesis of Peptide Substrates. The syntheses of linear GPA heptapeptide precursors based on the sequences of teicoplanin and vancomycin were performed using established methods to generate purified peptide-coenzyme A (CoA) conjugates.[21, 41, 42] Specific amino acid sequences used in this study were NH_2-(D)-Hpg-(D)-Tyr-(L)-Hpg-(D)-Hpg-(D)-Hpg-(L)-Tyr-(D/L)-Hpg-CoA for the teicoplanin-like peptide (**1-CoA**) (Hpg – 4-hydroxyphenylglycine) and NH_2-(D)-Leu-(D)-Tyr-(L)-Asn-(D)-Hpg-(D)-Hpg-(L)-Tyr-(D/L)-Hpg-CoA for the vancomycin-like peptide (**2-CoA**) (Figure 2). Loading of peptidyl-CoA substrates onto carrier proteins was then performed as previously reported[19-22] using the promiscuous phosphopantetheinyl transferase Sfp (R4-4 mutant).[43]

Cytochrome P450 Activity Assay. The cyclization activities of the two OxyB hybrid enzymes that could be purified ($OxyB_{tei\_FGv}$ and $OxyB_{tei\_BC/FGv}$) were tested using

various combinations of carrier protein/ substrate peptide using reported assay conditions.[19-22] Briefly, 2μM of P450 enzyme was supplemented by redox partner proteins (5μM PuxB variant A105V and 1μM PuR)[44] and loaded PCP-peptide containing NRPS construct (50μM). The reaction was initiated by the addition of 2mM NADH (Gerbu, Biotechnik) which was continually regenerated using an NADH regeneration system (0.33% (w/v) glucose, 9 U/mL glucose dehydrogenase (Sorachim)). For each peptide/carrier protein combination tested, triplicate reactions were performed together with control reactions in which either the P450 enzyme or NADH was excluded from the reaction mixture. Reactions were incubated for 1 h (that we have previously shown to be sufficient for maximal P450-mediated activity to be observed)[18-20, 28] with gentle shaking at 30°C, before being quenched by the addition of methylamine (40 % (v/v), 32,000-fold molar excess over peptidyl-PCP), resulting in the formation of methylamide peptides. After incubation for 15 min at 20°C, the turnover mixture was neutralized on ice using dilute formic acid. The cleaved peptides were purified using solid phase extraction (Strata-X polymeric reversed phase (Phenomenex)) and analyzed by analytical HPLC-MS using a Shimadzu LCMS-2020 system additionally equipped with an SPD-20A Prominence Dual Wavelength UV Detector. The turnover reactions were analyzed on a Waters XBridge BEH 300 C_{18} column (5μm, 4.6 × 250mm) at a flow rate of 1.0 mL/min using the following gradient: 0-4 min 5% solvent B, 4-4.5 min up to 15% solvent B, 4.5-25 min up to 50% solvent B (Solvent A: water + 0.1% formic acid; Solvent B: HPLC-grade acetonitrile + 0.1% formic acid) using single ion monitoring in negative mode, with product formation based on the mass difference of two Dalton per crosslink introduced. The yield of monocyclic peptide produced in each reaction was determined as the proportion of integrated peak area corresponding to the monocyclic peptide product compared with that of the total integrated peptide area (i.e for linear and monocyclic peptide combined); this is expressed as a percentage value in Table 3.

Results and Discussion

Design of OxyB hybrid enzymes. One of the challenges in understanding the differences between the *in vitro* behavior of the GPA biosynthetic $OxyB_{van}$ and $OxyB_{tei}$ enzymes is the high degree of structural and sequence similarity these P450s share. The major differences in the structures of these homologues is found in regions of the active site above the heme moiety: specifically, the B-C loop, which is typically unstructured in the substrate free state and folds upon substrate binding to form one side of the P450 active site, and the F-G helices that form the roof of the active site.[19, 22, 29, 45] In the case of the Oxy proteins, the F-G helices also form the major site of interactions with the X-domain, although selectivity for specific P450/X-domain interactions appears focused on the conserved PRDD motif at the beginning of the F-helix.[19, 45] The

reasons for transplanting entire regions of the active site was to maintain potentially important interactions within these regions that would be lost in a strategy based around sequential mutations. Additionally, the effect of individual mutations on P450 expression and solubility can be significant – possibly also due to the loss of important short-range interactions that would otherwise be absent in the mutated protein. By selecting these regions, we also could assess how these regions effect peptide turnover in solution, which is not captured in the substrate free structures of these P450s to date.[17, 19, 22, 29, 46-50] Furthermore, modelling of the likely position of the PCP-bound peptide structure based on the structure of the $OxyB_{tei}$/X-domain complex[19] as well as related P450/PCP complexes[51] indicates that these two regions would be the most likely to interact with the PCP-domain.

We then designed three chimeric P450 proteins based on an $OxyB_{tei}$ template sequence, with the B-C region ($OxyB_{tei\_BCv}$), the F-G helices ($OxyB_{tei\_FGv}$) or both regions ($OxyB_{tei\_BC/FGv}$) altered to the sequences from the vancomycin homologue (Figure 3). We chose to use the $OxyB_{tei}$ homologue as the template to determine whether any chimeric protein displayed gain of function, as opposed to a loss of function that could be difficult to attribute to specific alterations in protein structure. In the BC loop region, the sequences differ in 6 out of 39 residues (15%: K59Q, R60Q, F67W, R69P, T76K, V78I), with the most significant difference the R69P mutation. Overall, the changes contribute to an increase in the aliphatic index of the sequence (44.87 to 47.44) and reduce the number of charged residues by 2. In the FG region, the sequences differ in 14 out of 45 residues (31%: Q164R, A165D, L167M, Q168K, R172G, A180Q, R181K, K182R, A186L, E188D, A189K, A191S, V195L, M198I), with many being conservative substitutions; overall the actual hydrophobicity of this region decreases (aliphatic index changes from 72.00 to 71.78) and there is an increase in charged residues from 5 negative/ 9 positive residues to 6 negative/ 11 positive residues in the $OxyB_{van}$ sequence. Thus, our anticipation was that the $OxyB_{tei\_BCv}$ sequence was most likely to cause issues with soluble expression due to the increase in hydrophobicity of the BC loop region in this construct.

Expression, purification and characterization of OxyB hybrid enzymes. The sequences for the three chimeric P450s were then obtained as synthetic genes with codon usage and GC% content optimized for *E. coli* expression, with the reduction in GC% content from the native sequences especially important for ease of cloning and subsequent modification due to the high GC% content of the producer strains. The constructs were cloned into pET28a expression vectors, which resulted in constructs bearing an N-terminal His_6-tag together with a thrombin protease cleavage site. Expression of all constructs was tested in both LB and TB media, with a reduction in temperature to 18°C and supplementation of the heme precursor δ-aminolevulinic acid upon IPTG induction (0.1 mM) at a relatively high optical density (OD_{600} ~ 1.0). Purification of the expressed

proteins was executed as was performed for the wildtype proteins, using a combination of Ni-NTA affinity, ion exchange and gel filtration chromatography. Initial concerns about the $OxyB_{tei\_BCv}$ proved well founded, with purification of this construct failing at the Ni-NTA affinity stage due to protein aggregation upon elution from the Ni-NTA affinity column. In the case of the other hybrid OxyB proteins, both could be successfully purified using the standard three-step process and that afforded yields that were comparable to wildtype $OxyB_{tei}$ (170 nmol/L; TB media) for the $OxyB_{tei\_FGv}$ hybrid (160 nmol/L; LB media) or slightly reduced for the $OxyB_{tei\_BC/FGv}$ hybrid (110 nmol/L, TB media). Thus, in the case of the $OxyB_{tei\_BC/FGv}$ hybrid, the change in sequence of the FG helices appears to be sufficient to counteract the increased hydrophobicity of the BC loop region from the $OxyB_{van}$ sequence. Both purified hybrid enzymes also displayed levels of heme incorporation and CO difference spectra for both purified hybrids also demonstrated that the thiolate ligation state of both hybrid P450s was intact, with very little of the protonated, P420 state visible (Figure 4).

Structural analysis of the $OxyB_{tei\_BC/FGv}$ hybrid. In order to determine that there had been no major changes in structure of these hybrid enzymes we determined the structure of the most significantly altered hybrid – the $OxyB_{tei\_BC/FGv}$ hybrid – by X-ray crystallography to a resolution of 2.5 Å (Table 1). Phasing was accomplished using the structure of the parental P450, $OxyB_{tei}$ (PDB Code 4TVF),[22] followed by iterations of manual building in Coot and refinement using Phenix. The structure of the $OxyB_{tei\_BC/FGv}$ hybrid retains the classic P450-fold with no major obvious alterations, and closely resembles the parent $OxyB_{tei}$ structure (RMSD 1.0 Å) [22] as well as related OxyB enzymes $OxyB_{van}$ (RMSD 0.9-1.1 Å)[29] and StaH (RMSD 1.2 Å) (Figure 5).[17] Structural similarity to examples of the other three Oxy proteins (OxyA, OxyC and OxyE)[28, 46, 48-50] also shows high levels of structural similarity (RMSD 1.6-2.4 Å), which is characteristic for members of the CYP165 family and likely stems from their large peptide substrates and interaction with both the peptide-bound carrier protein domain as well as the unique X-domain NRPS-recruitment platform via a conserved PRDD motif at the beginning of the F-helix. [19, 45]

The $OxyB_{tei\_BC/FGv}$ hybrid also shows high levels of structural similarity to certain other bacterial P450s with large substrates and thus comparably large, open active sites[52-54] as well as structural similarity to P450s that have been shown to accept carrier protein bound substrates ($P450_{BioI}$ – *fattyacyl*-ACP; OxyD/Sky32 – *aminoacyl*-PCP) (Table 2). [51, 55-57] Comparing the active site regions of the $OxyB_{tei\_BC/FGv}$ hybrid with the parent $OxyB_{tei}$ structure shows that these are highly similar for all regions, including the BC loop region although more residues are visible in the structure of the hybrid. The FG helices are also in a very similar orientation in both structures, although they move slightly towards the BC loop region of the active site in the structure of the $OxyB_{tei\_BC/FGv}$ hybrid. The FG helices in complex with the X-domain adopt a conformation more

closely related to that seen in the $OxyB_{tei\_BC/FGv}$ hybrid, whilst in all cases the orientation of the essential PRDD X-domain interaction motif found at the start of the F-helix is unchanged. The only major difference between the structures of the $OxyB_{tei\_BC/FGv}$ hybrid and $OxyB_{tei}$ is found at the junction of the C- and D-helices, which occurs as a result of differences in the crystal packing observed in each case. Comparing the active site of the $OxyB_{tei\_BC/FGv}$ hybrid with the those of StaH and $OxyB_{van}$, only minor differences can be observed: in the case of $OxyB_{van}$, the FG helices orientation matches the hybrid well, whilst the N-terminus of the BC loop in $OxyB_{van}$ closes over the active site heme in a manner not observed for any other OxyB structure determined to date. When comparing the $OxyB_{tei\_BC/FGv}$ hybrid to StaH, the major differences are a difference in conformation of the connecting loop of the FG helices and the fact that all of the BC loop is visible in this structure; non-the-less the visible regions of the $OxyB_{tei\_BC/FGv}$ hybrid BC loop match the structure of the StaH BC loop well. Thus, from a structural perspective it is clear that the $OxyB_{tei\_BC/FGv}$ hybrid adopts a classic Oxy-type P450 structure and that the active site has not been distorted or otherwise effected by the alterations of both the BC and FG regions of the active site. Given that there is little structural difference between the parent $OxyB_{tei}$ and $OxyB_{van}$ homologues however, an assessment of the activity of the hybrid OxyB enzymes was now required in order to assess the effects of the active site alterations introduced into these enzymes.

Catalytic activity of the $OxyB_{tei\_FGv}$ and $OxyB_{tei\_BC/FGv}$ hybrids. With the purified OxyB hybrid enzymes in hand, we then characterized their peptide cyclization properties against model teicoplanin type (**1**) and vancomycin-type (**2**) heptapeptides. Both model peptides contained a *rac* 7-Hpg residue, whilst the teicoplanin type heptapeptide also contained a 3-Hpg residue for reasons of synthetic ease and consistency with previous experiments.[19-21] The peptides were synthesized as their CoA-thioesters using previously reported conditions, before being subsequently loaded onto carrier protein domains. For this study three different NRPS constructs were chosen as probes for each of the P450 enzymes: a di-domain PCP_7-X protein from teicoplanin biosynthesis[19, 20] and single PCP_7 domains from complestatin[21, 58] and teicoplanin/chloroerymomycin biosynthesis machineries (indicated as tei, com and cep, respectively).[19, 22] These constructs were chosen based on their use in previous turnover experiments that clearly showed the $OxyB_{van}$ homologue displaying not only superior activity in cyclizing peptides on the PCP-X protein irrespective of peptide sequence but displaying high levels of activity when peptides were presented by isolated PCP domains.[19, 20, 22] Thus, comparative turnovers of these two peptides on the three NRPS proteins selected would allow us to assess whether the properties of the OxyB hybrid proteins had been altered from that of the parental $OxyB_{tei}$ enzyme. In OxyB-catalyzed cyclization experiments supported by previously established redox partners (PuR and mutated PuxB)[44] we firstly determined that both OxyB hybrid enzymes retain

their catalytic activity against teicoplanin-type heptapeptides when presented on the PCP-X_{tei} construct, with levels of activity the same as those of the parent $OxyB_{tei}$ enzyme.[19, 20] Assessment of the activity of the hybrid enzymes against teicoplanin-peptides bound to isolated PCP domains showed that the incorporation of $OxyB_{van}$ active site regions was not sufficient to overcome the inability of $OxyB_{tei}$ to process these substrates effectively, with the yield of cyclized peptide actually reduced over those of the $OxyB_{tei}$ parent. The incorporation of the $OxyB_{van}$ active site regions was also not enough to promote the acceptance of the vancomycin-type peptide by either hybrid, either with or without X-domain containing constructs. Curiously, the only significant difference between the activity profiles of the two hybrid enzymes was found in the turnover of vancomycin-type peptides when bound to PCP_7-X_{tei}, in which the $OxyB_{tei\_BC/FGv}$ hybrid showed twice the activity of the $OxyB_{tei\_FGv}$ hybrid; however, as even the yield of the $OxyB_{tei\_BC/FGv}$ hybrid was below that of the template $OxyB_{tei}$ enzyme, it is unclear as to what extent the altered active site regions found in this hybrid have been able to counteract the apparent disruption of the active sites of these hybrid enzymes (Figure 6/Table 3).

In conclusion, we have shown that hybrid P450 OxyB enzymes from the glycopeptide antibiotic cyclization cascade can be successfully generated via the exchange of complete secondary structure regions surrounding the active site. The properties of these hybrid OxyB enzymes compare well with those of the parental P450 taken as a template for these experiments. We could determine the crystal structure of one of these hybrid P450 enzymes, which showed a high degree of similarity to that of the parental P450 and only minor differences in the active site regions that were match the sequence of the other parental P450. Furthermore, these results show that the unusual *in vitro* behavior of the OxyB homologue from the vancomycin does not stem from the major regions of the P450 active site, and that additional regions in and around the P450 active site must contribute to the unusual properties of this P450 enzyme.

Funding Sources

This work was supported by the Deutsche Forschungsgemeinschaft (Emmy−Noether Program, CR 392/1-1 (M.J.C)), Monash University & EMBL Australia (M.J.C). This research was supported under Australian Research Council's *Discovery Projects* funding scheme (project number DP170102220) to M.J.C.. M.J.C. would also like to acknowledge the support of the National Health and Medical Research Council through the provision of a Career Development Fellowship (APP1140619).

Acknowledgements

G. Stier (BZH-Heidelberg) for fusion protein vectors; S. Bell (University of Adelaide) for redox proteins; J. Yin (University of Chicago) for the R4-4 Sfp expression plasmid; A. Weinmann (MPIMF) for assistance in cloning and protein preparation; M. Müller (MPIMF) for mass spectral analysis; C. Roome (MPIMF) for IT support; and I. Schlichting (MPIMF) for constant support, encouragement and mentorship.

Table of Abbreviations

cep - chloroeremomycin

com – complestatin

GPA – glycopeptide antibiotic

Hpg – 4-hydroxyphenylglycine

NRPS – non-ribosomal peptide synthetase

NTA – nitrilotriacetic acid agarose resin

Oxy – Cytochrome P450 from glycopeptide antibiotic biosynthesis

PCP – peptidyl carrier protein

tei – teicoplanin

van – vancomycin

References

[1] D.J. Newman, G.M. Cragg, Journal of Natural Products, 75, 2012, 311-335.

[2] A. Greule, J.E. Stok, J.J. De Voss, M.J. Cryle, Nat. Prod. Rep, 2018 Apr 18. doi: 10.1039/c7np00063d.

[3] M.J.G. Elizabeth, A.H. Martin, Current Topics in Medicinal Chemistry, 13, 2013, 2254-2280.

[4] W. Huang, W.A. Johnston, M.A. Hayes, J.J. De Voss, E.M.J. Gillam, Arch. Biochem. Biophys., 467, 2007, 193-205.

[5] D.J.B. Hunter, J.B.Y.H. Behrendorff, W.A. Johnston, P.Y. Hayes, W. Huang, B. Bonn, M.A. Hayes, J.J. De Voss, E.M.J. Gillam, Metabolic Engineering, 13, 2011, 682-693.

[6] J.B.Y.H. Behrendorff, W.A. Johnston, E.M.J. Gillam, in: E.M.J. Gillam, J.N. Copp, D. Ackerley (Eds.), Directed Evolution Library Creation: Methods and Protocols, Springer New York, New York, NY, 2014, pp. 175-187.

[7] W.A. Johnston, W. Huang, J.J. De Voss, M.A. Hayes, E.M.J. Gillam, Drug Metabolism and Disposition, 35, 2007, 2177-2185.

[8] J.B.Y.H. Behrendorff, C.D. Moore, K.-H. Kim, D.-H. Kim, C.A. Smith, W.A. Johnston, C.-H. Yun, G.S. Yost, E.M.J. Gillam, Chemical Research in Toxicology, 25, 2012, 1964-1974.

[9] R.S. Al Toma, C. Brieke, M.J. Cryle, R.D. Suessmuth, Nat. Prod. Rep., 32, 2015, 1207-1235.

[10] G. Yim, M.N. Thaker, K. Koteva, G. Wright, J. Antibiot., 67, 2014, 31-41.

[11] M.S. Butler, K.A. Hansford, M.A.T. Blaskovich, R. Halai, M.A. Cooper, J. Antibiot., 67, 2014, 631-644.

[12] B. Hadatsch, D. Butz, T. Schmiederer, J. Steudle, W. Wohlleben, R. Suessmuth, E. Stegmann, Chem. Biol., 14, 2007, 1078-1089.

[13] E. Stegmann, S. Pelzer, D. Bischoff, O. Puk, S. Stockert, D. Butz, K. Zerbe, J. Robinson, R.D. Suessmuth, W. Wohlleben, J. Biotech., 124, 2006, 640-653.

[14] M. Peschke, C. Brieke, M. Heimes, M.J. Cryle, ACS Chem. Biol., 13, 2018, 110-120.

[15] K. Haslinger, C. Redfield, M.J. Cryle, Proteins: Struct., Funct., Bioinf., 83, 2015, 711-721.

[16] M. Peschke, C. Brieke, R.J. Goode, R.B. Schittenhelm, M.J. Cryle, Biochemistry, 56, 2017, 1239-1247.

[17] V. Ulrich, M. Peschke, C. Brieke, M.J. Cryle, Mol. BioSys., 12, 2016, 2992-3004.

[18] M. Peschke, K. Haslinger, C. Brieke, J. Reinstein, M. Cryle, J. Am. Chem. Soc., 138, 2016, 6746-6753.

[19] K. Haslinger, M. Peschke, C. Brieke, E. Maximowitsch, M.J. Cryle, Nature, 521, 2015, 105-109.

[20] C. Brieke, M. Peschke, K. Haslinger, M.J. Cryle, Angew. Chem., Int. Ed., 54, 2015, 15715-15719.

[21] C. Brieke, V. Kratzig, K. Haslinger, A. Winkler, M.J. Cryle, Org. Biomol. Chem., 13, 2015, 2012-2021.

[22] K. Haslinger, E. Maximowitsch, C. Brieke, A. Koch, M.J. Cryle, ChemBioChem, 15, 2014, 2719-2728.

[23] P.C. Schmartz, K. Wolfel, K. Zerbe, E. Gad, E. El Tamany, H.K. Ibrahim, K. Abou-Hadeed, J.A. Robinson, Angew. Chem.-Int. Edit., 51, 2012, 11468-11472.

[24] N. Geib, K. Woithe, K. Zerbe, D.B. Li, J.A. Robinson, Bioorg. Med. Chem. Lett., 18, 2008, 3081-3084.

[25] K. Woithe, N. Geib, K. Zerbe, D.B. Li, M. Heck, S. Fournier-Rousset, O. Meyer, F. Vitali, N. Matoba, K. Abou-Hadeed, J.A. Robinson, J. Am. Chem. Soc., 129, 2007, 6887-6895.

[26] K. Zerbe, K. Woithe, D.B. Li, F. Vitali, L. Bigler, J.A. Robinson, Angew. Chem., Int. Ed., 43, 2004, 6709-6713.

[27] J. Tailhades, M. Schoppet, A. Greule, M. Peschke, C. Brieke, M.J. Cryle, Chemical Communications, 54, 2018, 2146-2149.

[28] M. Peschke, C. Brieke, M. Cryle, Sci. Rep., 6, 2016, 35584.

[29] K. Zerbe, O. Pylypenko, F. Vitali, W. Zhang, S. Rouset, M. Heck, J.W. Vrijbloed, D. Bischoff, B. Bister, R.D. Sussmuth, S. Pelzer, W. Wohlleben, J.A. Robinson, I. Schlichting, J. Biol. Chem., 277, 2002, 47476-47485.

[30] W. Kabsch, Acta Crystallogr. D, 66, 2010, 125-132.

[31] A.J. McCoy, R.W. Grosse-Kunstleve, P.D. Adams, M.D. Winn, L.C. Storoni, R.J. Read, J. Applied Crystallogr., 40, 2007, 658-674.

[32] P. Emsley, B. Lohkamp, W.G. Scott, K. Cowtan, Acta Crystallogr. D, 66, 2010, 486-501.

[33] P. Emsley, K. Cowtan, Acta Crystallogr. D, 60, 2004, 2126-2132.

[34] P.D. Adams, P.V. Afonine, G. Bunkoczi, V.B. Chen, I.W. Davis, N. Echols, J.J. Headd, L.-W. Hung, G.J. Kapral, R.W. Grosse-Kunstleve, A.J. McCoy, N.W. Moriarty, R. Oeffner, R.J. Read, D.C. Richardson, J.S. Richardson, T.C. Terwilliger, P.H. Zwart, Acta Crystallogr. D, 66, 2010, 213-221.

[35] V.B. Chen, W.B. Arendall, J.J. Headd, D.A. Keedy, R.M. Immormino, G.J. Kapral, L.W. Murray, J.S. Richardson, D.C. Richardson, Acta Crystallogr. D, 66, 2010, 12-21.

[36] E. Krissinel, K. Henrick, Acta Crystallogr. D, 60, 2004, 2256-2268.

[37] L. Holm, P. Rosenström, Nucleic Acids Res., 38, 2010, W545-W549.

[38] F. Sievers, A. Wilm, D. Dineen, T.J. Gibson, K. Karplus, W. Li, R. Lopez, H. McWilliam, M. Remmert, J. Söding, J.D. Thompson, D.G. Higgins, Molecular Systems Biology, 7, 2011.

[39] G. E., H. C., G. A., D. S., W. M.R., A. R.D., B. A., in: J.M. Walker (Ed.), The Proteomics Protocols Handbook, Humana Press, 2005, pp. 571-607.

[40]

[41] C. Brieke, V. Kratzig, M. Peschke, M.J. Cryle, in: S.B. Evans (Ed.), Nonribosomal Peptide and Polyketide Biosynthesis: Methods and Protocols, Springer New York, New York, NY, 2016, pp. 85-102.

[42] C. Brieke, M.J. Cryle, Org. Lett., 16, 2014, 2454-2457.

[43] M. Sunbul, N.J. Marshall, Y. Zou, K. Zhang, J. Yin, J. Mol. Biol., 387, 2009, 883-898.

[44] S.G. Bell, A.B.H. Tan, E.O.D. Johnson, L.-L. Wong, Mol. BioSys., 6, 2009, 206-214.

[45] M. Peschke, M. Gonsior, R.D. Süssmuth, M.J. Cryle, Curr. Opin. Struct. Biol., 41, 2016, 46-53.

[46] V. Ulrich, C. Brieke, M.J. Cryle, Beilstein Journal of Organic Chemistry, 12, 2016, 2849-2864.

[47] K. Haslinger, M. Cryle, FEBS Lett., 590, 2016, 571-581.

[48] Z. Li, S.G. Rupasinghe, M.A. Schuler, S.K. Nair, Proteins: Struct., Funct., Bioinf., 79, 2011, 1728-1738.

[49] M.J. Cryle, J. Staaden, I. Schlichting, Arch. Biochem. Biophys., 507, 2011, 163-173.

[50] O. Pylypenko, F. Vitali, K. Zerbe, J.A. Robinson, I. Schlichting, J. Biol. Chem., 278, 2003, 46727-46733.

[51] K. Haslinger, C. Brieke, S. Uhlmann, L. Sieverling, R.D. Süssmuth, M.J. Cryle, Angew. Chem., Int. Ed., 53, 2014, 1-6.

[52] Y. Yasutake, N. Imoto, Y. Fujii, T. Fujii, A. Arisawa, T. Tamura, Biochemical and Biophysical Research Communications, 361, 2007, 876-882.

[53] K.J. McLean, M. Hans, B. Meijrink, W.B. van Scheppingen, A. Vollebregt, K.L. Tee, J.-M. van der Laan, D. Leys, A.W. Munro, M.A. van den Berg, Proceedings of the National Academy of Sciences of the United States of America, 112, 2015, 2847-2852.

[54] L.-H. Xu, S. Fushinobu, H. Ikeda, T. Wakagi, H. Shoun, J. Bacteriol., 191, 2009, 1211-1219.

[55] M.J. Cryle, I. Schlichting, PNAS, 105, 2008, 15696-15701.

[56] S. Uhlmann, R.D. Süssmuth, M.J. Cryle, ACS Chem. Biol., 8, 2013, 2586-2596.

[57] M.J. Cryle, A. Meinhart, I. Schlichting, J. Biol. Chem., 285, 2010, 24562-24574.

[58] A. Mollo, A.N. von Krusenstiern, J.A. Bulos, V. Ulrich, K.S. Akerfeldt, M.J. Cryle, L.K. Charkoudian, RSC Advances, 7, 2017, 35376-35384.

Table 1. Crystallographic data for $OxyB_{tei\_BC/FGv}$ hybrid

Data Collection	$OxyB_{tei\_BC/FGv}$ Native
Space Group	*P*1
Cell Dimensions *a, b, c* (Å) *x, y, z* (°)	 59.3, 83.2, 92.2; 85.20, 101.98, 97.83.
Molecules / asymmetric unit	4
X-ray source	PXII-X10SA, SLS
Wavelength (Å)	0.99991
Resolution (Å) [a]	50.0 – 2.5
No. of observed reflections	199449 (22758)
No. of unique reflections	57549 (6375)
Completeness (%) [a]	97.5 (97.0)
Redundancy	3.5 (3.6)
R_{merge} (%) [a]	7.3 (46.2)
$I/\sigma I$ [a]	11.3 (3.0)
$CC_{1/2}$ (%) [a,b]	99.7 (84.8)
Wilson *B*-factor (Å^2)	53.27
Refinement	
No. of reflections	57545
No. of reflections in test set	2877
Resolution in Refinement	48.26 – 2.50
R_{work} / R_{free} [c](%)	18.8/ 24.6
No. of non-H atoms Protein Heme Water/ ion Total	 11503 172 148 11823
B-factors Protein Heme Water/ ion Average	 59.9 29.7 44.5 59.3
RMSD Bond lengths (Å) Bond angles (°) Ramachandran statistics [d] Rotamer outliers [d]	 0.009 1.024 97.5/ 2.5/ 0 0.7
PDB Code	6FSH

[a] Numbers in parentheses correspond to the highest resolution shell (2.6–2.5 Å).

[b] As implemented in XDS [27]

[c] $R_{work} = \sum ||F_o|-|F_c|| / \sum|F_o|$, calculated from the working reflection set; R_{free} calculated in the same manner using the 5% test set reflections.

[d] Calculated by Molprobity;[35] percentage of the protein residues in most favored; allowed, disallowed regions and percentage of bad rotamers.

Table 2: Top ranking and carrier-protein interacting P450 structures with high levels of homology to the $OxyB_{tei\_BC/FGv}$ structure identified by Dali.[37]

PDB code	Chain	Z-score	RMSD Cα [Å]	% Identity	Description	Ref
4TX3	A	56.6	1.0	92	$OxyB_{tei}$-X-domain complex (*Actinoplanes teichomyceticus*)	[19]
5EX6	C	55.9	1.2	76	StaH (*Streptomyces toyocaensis*)	[17]
1LG9	A	55.1	0.9	73	$OxyB_{van}$ (*Amycolatopsis orientalis*)	[29]
1LFK	A	53.8	1.1	73		
1LGF	A	52.6	0.9	73		
4TVF	A	52.5	1.0	92	$OxyB_{tei}$ (*Actinoplanes teichomyceticus*)	[22]
1UED	A	48.7	1.6	49	$OxyC_{van}$ (*Amycolatopsis orientalis*)	[50]
2Z36	A	44.4	2.3	33	MoxA (Cyp105, *Nonomuraea recticatena*)	[52]
4OQS	A	44.1	2.1	40	CYP105AS1 (*Amycolatopsis orientalis*)	[53]
3E5L	A	44.0	2.5	37	CYP105P1 (*Streptomyces avermitilis*)	[54]
3OO3	A	44.0	2.2	38	$OxyE_{tei}$ (CYP165D3, *Actinoplanes teichomyceticus*)	[48]
3O1A	A	43.6	2.3	38		[49]
5HH3	A	43.7	2.1	41	$OxyA_{tei}$ (*Actinoplanes teichomyceticus*)	[47]
5EX9	A	43.0	2.1	39	StaF (*Streptomyces toyocaensis*)	[46]
3EJE	F	39.4	2.7	29	$P450_{BioI}$ (CYP107H1, *Bacillus subtilis*)	[55]
4L0E	A	37.7	2.4	24	$P450_{sky}$ (CYP163B3, *Streptomyces* sp. ACTA 2897)	[56]
4PXH	A	37.4	3.2	24	PCP_7-$P450_{sky}$ complex (CYP163B3, *Streptomyces* sp. ACTA 2897)	[51]
4PWV	A	37.1	3.3	24		
3MGX	B	34.8	3.1	26	OxyD (*Amycolatopsis balhimycina*)	[57]

Table 3: Peptide crosslinking activity of OxyB hybrid enzymes generated in this study in comparison to previous result obtained with the parental OxyB homologues $OxyB_{tei}$ and $OxyB_{van}$.

Peptide	NRPS protein [a]	Cytochrome P450 activity (% crosslinked)			
		$OxyB_{van}$	$OxyB_{tei}$	$OxyB_{tei\_FGv}$	$OxyB_{tei\_BC/FGv}$
Teicoplanin-type (**1**)	PCP7-X_{tei}	72.3 +/- 4.9	65.7+/- 1.4	60.4 +/- 3.6	63.8 +/-4.3
	$PCP7_{com}$	87.2 +/- 2.7	ND	3.6 +/- 1.5	2.0 +/- 1.0
	$PCP7_{tei/cep}$	82.0 +/- 0.9 cep	28.0 +/- 1.0	8.3 +/- 2.1	6.1 +/- 2.9
Vancomycin-type (**2**)	PCP7-X_{tei}	94.5 +/- 1.8	38.4 +/- 2.8	11.5 +/- 2.1	20.5 +/- 1.9
	$PCP7_{com}$	92.3 +/- 1.1	ND	0.4 +/- 0.2	1.0 +/- 0.5
	$PCP7_{tei/cep}$	91.9 +/- 1.8 cep	ND	0.8 +/- 0.6	1.4 +/- 0.6

[a] Subscript indicates the NRPS machinery from which the constructs are derived: tei – teicoplanin biosynthesis, com – complestatin biosynthesis, cep – chloroeremomycin biosynthesis).

Figure 1. Structures of clinically relevant GPAs teicoplanin and vancomycin (**A**). Biosynthesis of GPAs – as shown for teicoplanin – is accomplished via initial peptide synthesis by a linear non-ribosomal peptide synthetase (NRPS) followed by a Cytochrome-P450 (Oxy)-meditated cyclization cascade to form the crosslinked, active antibiotic core of the GPAs. P450-mediated cyclization of the peptide occurs whilst the peptide remains bound to the final peptidyl carrier protein (PCP)-domain of the NRPS machinery,[14, 15] with the P450 enzymes recruited to the substrate through their interactions with the unique, adjacent X-domain. Cleavage of the completed peptide then triggers the actions of further modification enzymes responsible for addition of moieties such as sugars, fatty acids and sulfate groups. (**B**). Domain key: A – adenylation, C – condensation, E –

epimerization, PCP – peptidyl carrier protein, TE – Type-I thioesterase, X – P450 recruitment, Oxy – Cytochrome P450.

Figure 2. GPA heptapeptides used in this study: teicoplanin-type sequence (R = OH, **1**) and vancomycin-type sequence (R = OH, **2**) were synthesized as their CoA-thioesters (R = CoA, **1-CoA** / **2-CoA**) prior to carrier protein loading catalyzed by the phosphopantetheinyl transferase Sfp.

Figure 3. Sequence alignment of both parental OxyB homologues as well as the three hybrid proteins generated in this study. Secondary structure is shown and colored as in Figure 5A, with the regions of altered sequence boxed.

Figure 4. UV/Visible absorption spectra (black) and reduced, CO-complex (grey) shown for the hybrid proteins $OxyB_{tei\_FGv}$ (left panel) and $OxyB_{tei\_BC/FGv}$ (right panel).

Figure 5. Structure of $OxyB_{tei\_BC/FGv}$ hybrid (**A**); secondary structure elements are labeled and colored gray with the exceptions as follows: B-helix and loop region (magenta), D-helix (cherry red), E-helix (blue), F-helix (orange), G-helix (yellow), I-helix (cyan), β1-sheet (green), β2-sheet (purple), heme shown as sticks (C-atoms – red, N-atoms – blue, O-atoms – orange) with the heme iron shown as a red sphere. Overlays with related OxyB homologues (**B**); $OxyB_{tei\_BC/FGv}$ hybrid colored gray except for the BC loop and FG helices, which are colored green; $OxyB_{tei}$ colored orange, $OxyB_{van}$ colored magenta, StaH colored yellow.

Figure 6. Workflow of OxyB-catalyzed turnover experiments shown for peptide **1**. Initial peptide loading of the peptidyl-CoA onto the relevant carrier protein construct is performed using Sfp, after which the different OxyB homologues were tested for their ability to install the C-*O*-D crosslink into the loaded peptide. Following the reaction, the peptides are cleaved from the carrier proteins using methylamine and analyzed by LCMS. Insert: OxyB activity against the different peptide/ carier protein constructs tested in this study, showing conclusively that the hybrid OxyB enzymes behavior closely matches that of the parent $OxyB_{tei}$ (results are displayed for each substrate from left to right in the order of $OxyB_{van}$, $OxyB_{tei}$, $OxyB_{tei\_FGv}$ and finally $OxyB_{tei\_BC/FGv}$).

Figure 1.

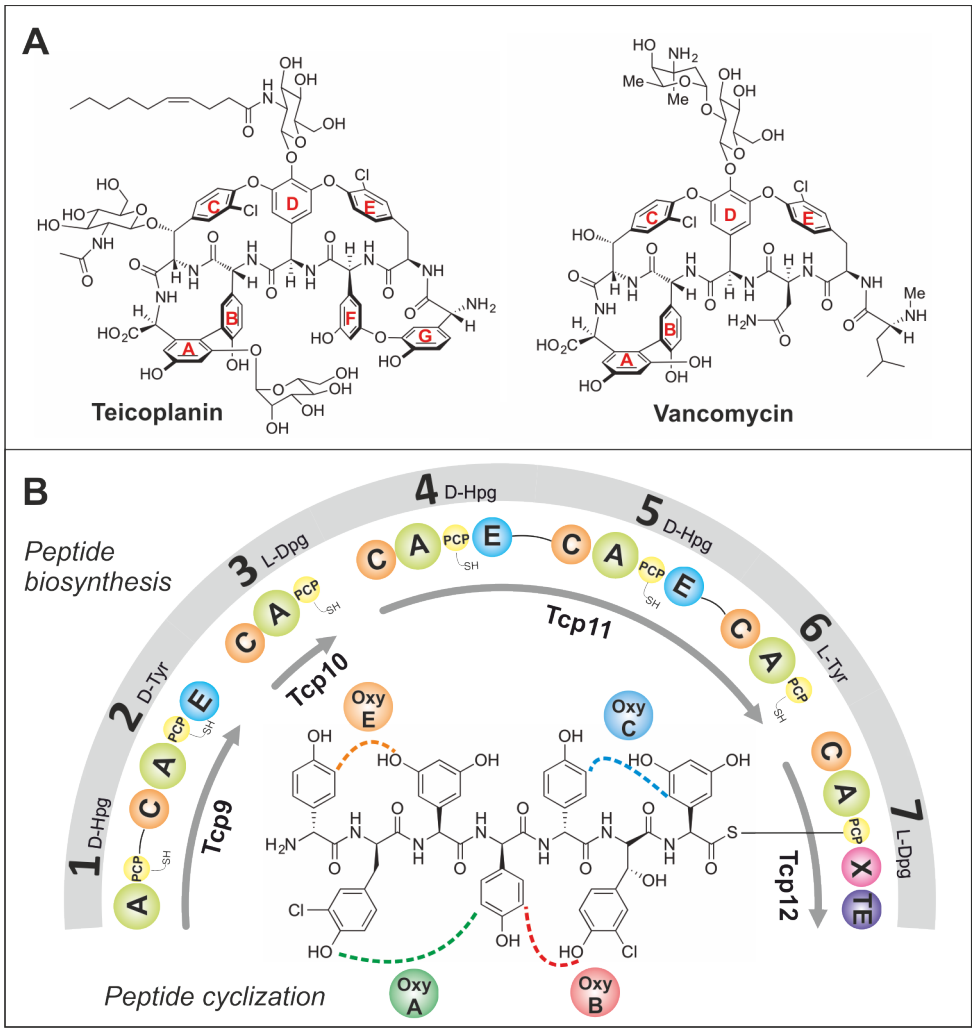
A
Teicoplanin
Vancomycin
B
Peptide biosynthesis
1 D-Hpg
2 D-Tyr
3 L-Dpg
4 D-Hpg
5 D-Hpg
6 L-Tyr
7 L-Dpg
Tcp9
Tcp10
Tcp11
Tcp12
Oxy A
Oxy B
Oxy C
Oxy E
Peptide cyclization

Figure 2.

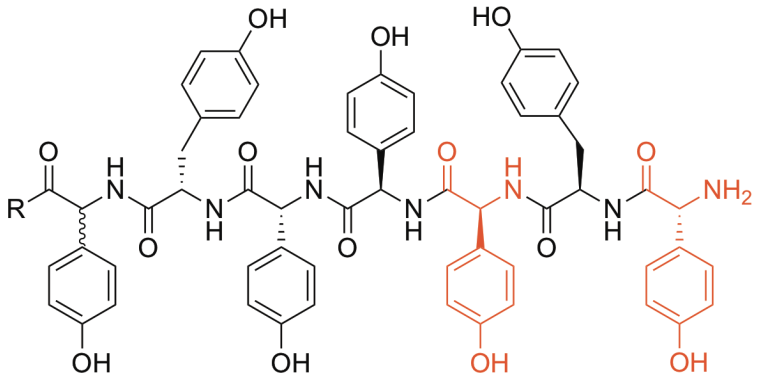

1

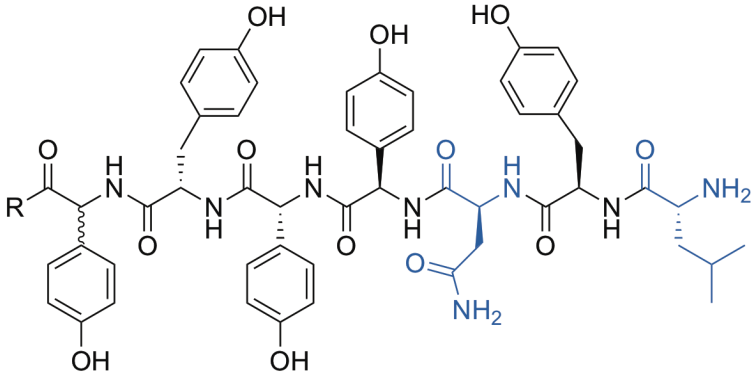

2

Figure 3.

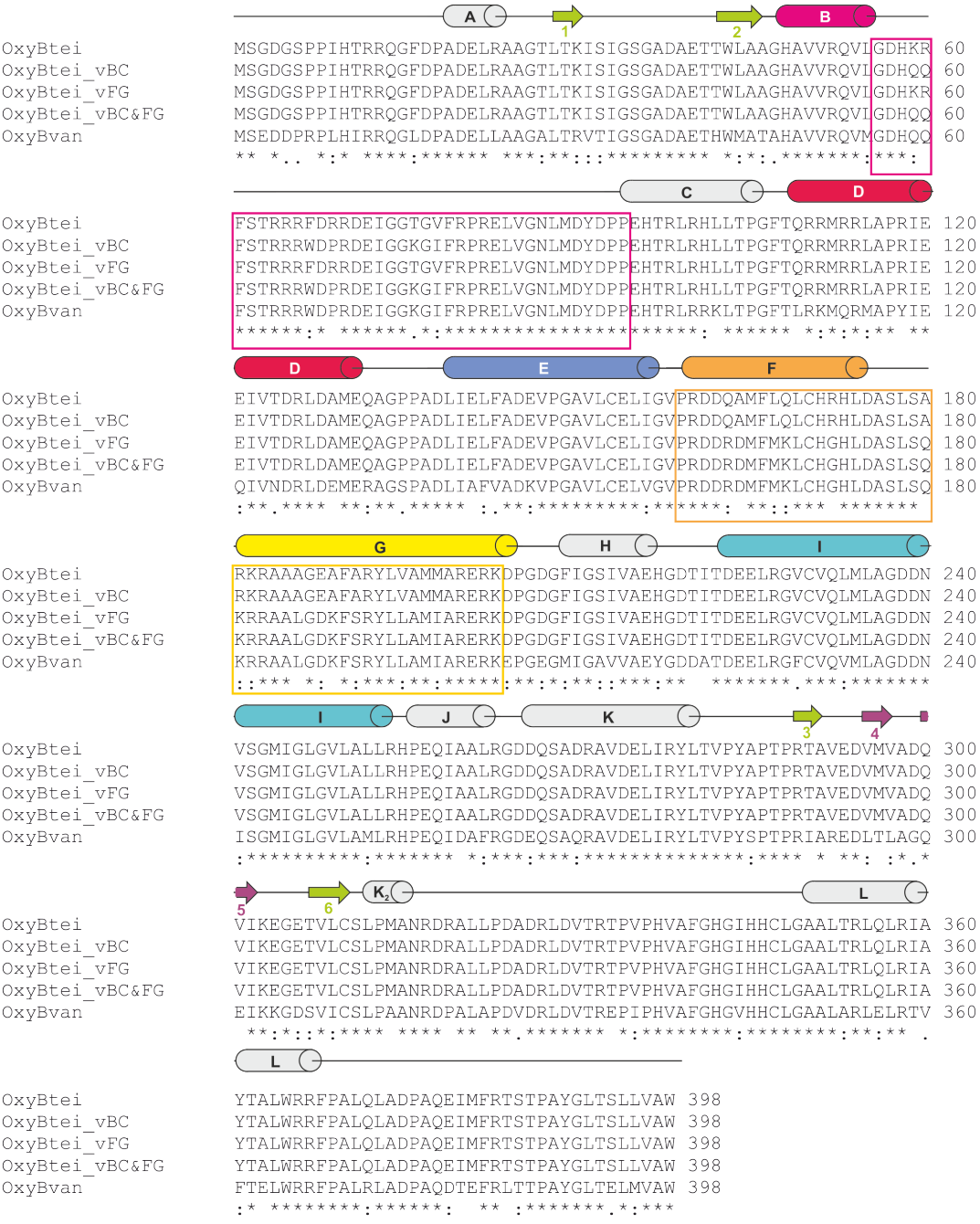
A
1
2
B
OxyBtei MSGDGSPPIHTRRQGFDPADELRAAGTLTKISIGSGADAETTWLAAGHAVVRQVLGDHKR 60
OxyBtei_vBC MSGDGSPPIHTRRQGFDPADELRAAGTLTKISIGSGADAETTWLAAGHAVVRQVLGDHQQ 60
OxyBtei_vFG MSGDGSPPIHTRRQGFDPADELRAAGTLTKISIGSGADAETTWLAAGHAVVRQVIGDHKR 60
OxyBtei_vBC&FG MSGDGSPPIHTRRQGFDPADELRAAGTLTKISIGSGADAETTWLAAGHAVVRQVIGDHQQ 60
OxyBvan MSEDDPRPLHIRRQGLDPADELLAAGALTRVTIGSGADAETHWMATAHAVVRQVMGDHQQ 60
C
D
OxyBtei FSTRRRFDRRDEIGGTGVFRPRELVGNLMDYDPPEHTRLRHLLTPGFTQRRMRRLAPRIE 120
OxyBtei_vBC FSTRRRWDPRDEIGGKGIFRPRELVGNLMDYDPPEHTRLRHLLTPGFTQRRMRRLAPRIE 120
OxyBtei_vFG FSTRRRFDRRDEIGGTGVFRPRELVGNLMDYDPPEHTRLRHLLTPGFTQRRMRRLAPRIE 120
OxyBtei_vBC&FG FSTRRRWDPRDEIGGKGIFRPRELVGNLMDYDPPEHTRLRHLLTPGFTQRRMRRLAPRIE 120
OxyBvan FSTRRRWDPRDEIGGKGIFRPRELVGNLMDYDPPEHTRLRRKLTPGFTLRKMQRMAPYIE 120
D
E
F
OxyBtei EIVTDRLDAMEQAGPPADLIELFADEVPGAVLCELIGVPRDDQAMFLQLCHRHLDASLSA 180
OxyBtei_vBC EIVTDRLDAMEQAGPPADLIELFADEVPGAVLCELIGVPRDDQAMFLQLCHRHLDASLSA 180
OxyBtei_vFG EIVTDRLDAMEQAGPPADLIELFADEVPGAVLCELIGVPRDDRDMFMKLCHGHLDASLSQ 180
OxyBtei_vBC&FG EIVTDRLDAMEQAGPPADLIELFADEVPGAVLCELIGVPRDDRDMFMKLCHGHLDASLSQ 180
OxyBvan QIVNDRLDEMERAGSPADLIAFVADKVPGAVLCELVGVPRDDRDMFMKLCHGHLDASLSQ 180
G
H
I
OxyBtei RKRAAAGEAFARYLVAMMARERKDPGDGFIGSIVAEHGDTITDEELRGVCVQLMLAGDDN 240
OxyBtei_vBC RKRAAAGEAFARYLVAMMARERKDPGDGFIGSIVAEHGDTITDEELRGVCVQLMLAGDDN 240
OxyBtei_vFG KRRAALGDKFSRYLLAMIARERKDPGDGFIGSIVAEHGDTITDEELRGVCVQLMLAGDDN 240
OxyBtei_vBC&FG KRRAALGDKFSRYLLAMIARERKDPGDGFIGSIVAEHGDTITDEELRGVCVQLMLAGDDN 240
OxyBvan KRRAALGDKFSRYLLAMIARERKEPGEGMIGAVVAEYGDDATDEELRGFCVQVMLAGDDN 240
I
J
K
3
4
OxyBtei VSGMIGLGVLALLRHPEQIAALRGDDQSADRAVDELIRYLTVPYAPTPRTAVEDVMVADQ 300
OxyBtei_vBC VSGMIGLGVLALLRHPEQIAALRGDDQSADRAVDELIRYLTVPYAPTPRTAVEDVMVADQ 300
OxyBtei_vFG VSGMIGLGVLALLRHPEQIAALRGDDQSADRAVDELIRYLTVPYAPTPRTAVEDVMVADQ 300
OxyBtei_vBC&FG VSGMIGLGVLALLRHPEQIAALRGDDQSADRAVDELIRYLTVPYAPTPRTAVEDVMVADQ 300
OxyBvan ISGMIGLGVLAMLRHPEQIDAFRGDEQSAQRAVDELIRYLTVPYSPTPRIAREDLTLAGQ 300
5
6
K2
L
OxyBtei VIKEGETVLCSLPMANRDRALLPDADRLDVTRTPVPHVAFGHGIHHCLGAALTRLQLRIA 360
OxyBtei_vBC VIKEGETVLCSLPMANRDRALLPDADRLDVTRTPVPHVAFGHGIHHCLGAALTRLQLRIA 360
OxyBtei_vFG VIKEGETVLCSLPMANRDRALLPDADRLDVTRTPVPHVAFGHGIHHCLGAALTRLQLRIA 360
OxyBtei_vBC&FG VIKEGETVLCSLPMANRDRALLPDADRLDVTRTPVPHVAFGHGIHHCLGAALTRLQLRIA 360
OxyBvan EIKKGDSVICSLPAANRDPALAPDVDRLDVTREPIPHVAFGHGVHHCLGAALARLELRTV 360
L
OxyBtei YTALWRRFPALQLADPAQEIMFRTSTPAYGLTSLLVAW 398
OxyBtei_vBC YTALWRRFPALQLADPAQEIMFRTSTPAYGLTSLLVAW 398
OxyBtei_vFG YTALWRRFPALQLADPAQEIMFRTSTPAYGLTSLLVAW 398
OxyBtei_vBC&FG YTALWRRFPALQLADPAQEIMFRTSTPAYGLTSLLVAW 398
OxyBvan FTELWRRFPALRLADPAQDTEFRLTTPAYGLTELMVAW 398

Figure 4.

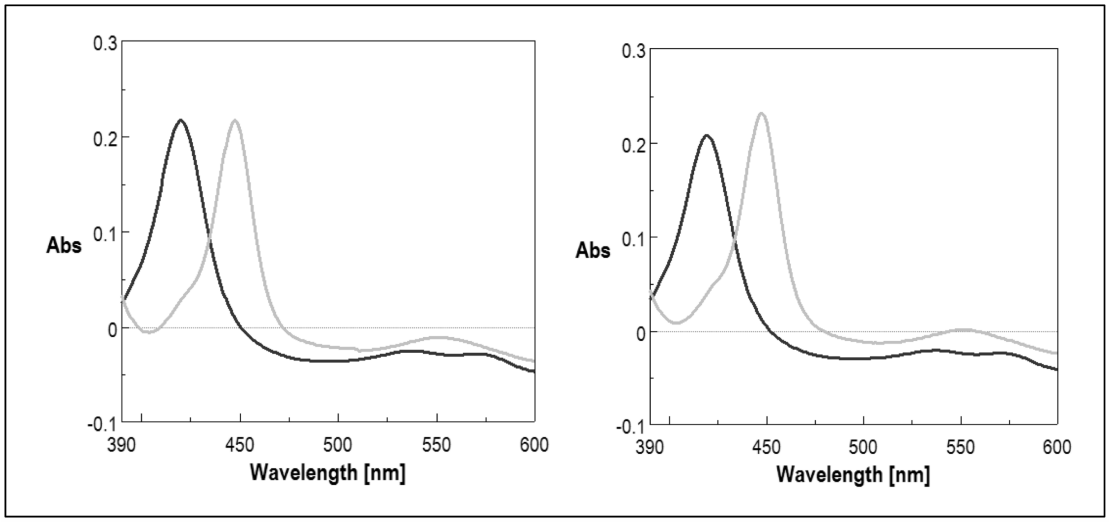
0.3
0.2
0.1
0
-0.1
Abs
390
450
500
550
600
Wavelength [nm]
0.3
0.2
0.1
0
-0.1
Abs
390
450
500
550
600
Wavelength [nm]

Figure 5.

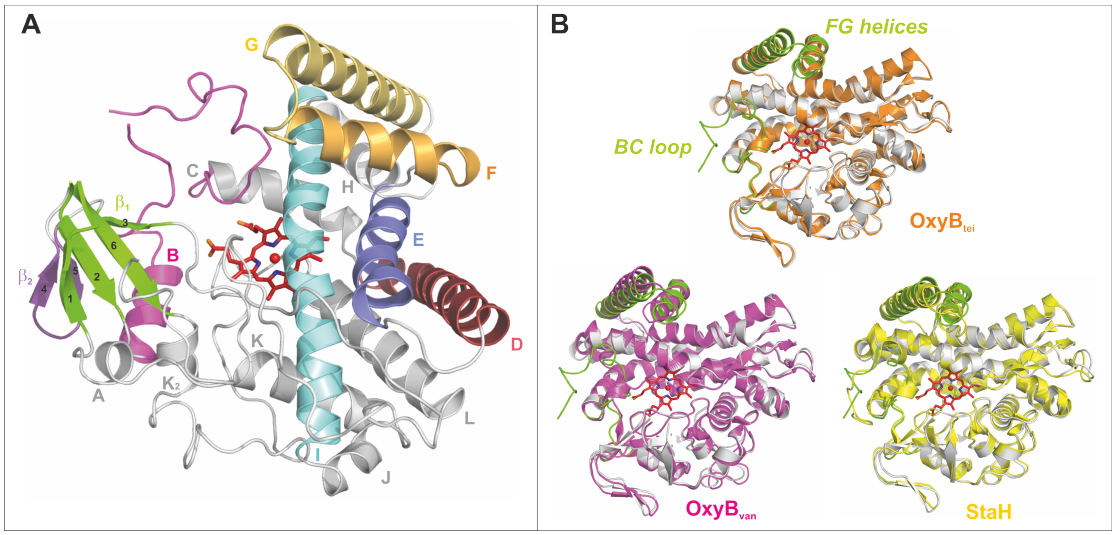
A
G
C
H
F
β1
3
6
B
E
β2
4
5
2
1
K
D
A
K2
L
I
J
B
FG helices
BC loop
OxyBtei
OxyBvan
StaH

Figure 6.

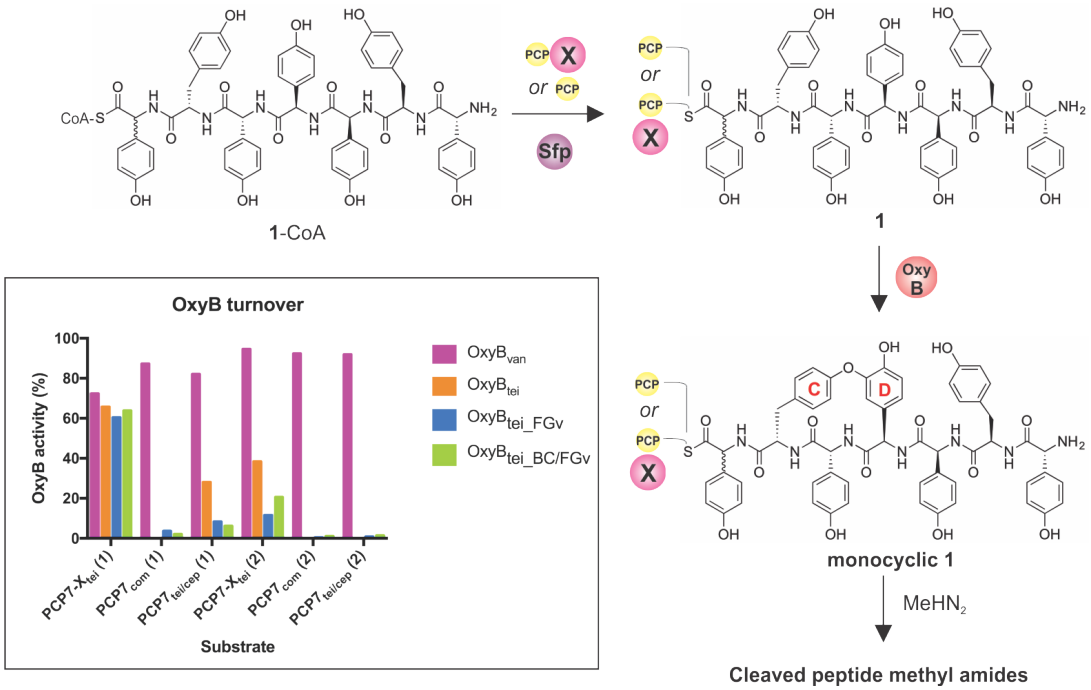
CoA-S
1-CoA
PCP
X
or
PCP
Sfp
PCP
or
PCP
X
1
Oxy B
C
D
monocyclic 1
MeHN2
Cleaved peptide methyl amides
OxyB turnover
OxyB activity (%)
100
80
60
40
20
0
OxyBvan
OxyBtei
OxyBtei_FGv
OxyBtei_BC/FGv
PCP7-Xtei (1)
PCP7 com (1)
PCP7 tei/cep (1)
PCP7-Xtei (2)
PCP7 com (2)
PCP7 tei/cep (2)
Substrate